



# Investigation of H<sub>2</sub> storage in a templated carbon derived from zeolite Y and PFA

C. Guan, X. Zhang, K. Wang\*, C. Yang

School of Chemical and Biomedical Engineering, Nanyang Technological University, Singapore 637459, Singapore

## ARTICLE INFO

### Article history:

Received 30 October 2008

Received in revised form 16 January 2009

Accepted 26 January 2009

### Keywords:

Template carbon  
Adsorption  
Hydrogen storage  
Activated carbon  
Characterization

## ABSTRACT

An activated carbon sample was synthesized using poly furfuryl alcohol (PFA) as the carbon precursor and ammonium-form zeolite Y as the template. The sample presents a specific surface area of 2545 m<sup>2</sup>/g and a hydrogen sorption capacity of 2.4% at 10 bar and 77 K. The structure of the sample was characterized with the sorption isotherms of N<sub>2</sub>, Ar, and CO<sub>2</sub>, respectively. It was found that the small micropores and the specific surface area were better characterized by CO<sub>2</sub> sorption and Ar sorption, respectively. The existence of the small micropores was confirmed by hydrogen isosteric heat of adsorption.

© 2009 Elsevier B.V. All rights reserved.

## 1. Introduction

Template synthesis is a promising technology for preparing activated carbon (AC) samples with large surface area and relatively uniform porous structure [1–6]. This kind of carbons (referred to as templated carbon or TC) has caught some recent research attention in the energy gas (H<sub>2</sub>) storage application, where the surface area, pore size and the microporosity dictate the uptake capacity [7,8]. A few recent studies have demonstrated the potential of TCs for H<sub>2</sub> storage. For example, Chen et al. [9] prepared a TC using zeolite Y as templates and propylene/butylene as carbon sources. The H<sub>2</sub> capacity was 2 wt% at 77 K and 1 bar. Armandi et al. [10] applied the post-treatments (activations) for TCs prepared using SBA-15 silica as template and reached a capacity of 2.0 wt% at 77 K and 1 bar. Yang et al. synthesized a TC via CVD process with zeolite  $\beta$  and acetonitrile. The H<sub>2</sub> capacity of 6.9 wt% was observed at 77 K and 20 bar [11]. A composite of TC-platinum nanoparticles reported a H<sub>2</sub> uptake of 1.35 wt% at 298 K and 100 bar [12]. Table 1 generalizes the synthetic methods and the related H<sub>2</sub> storage performance for a few TC samples.

H<sub>2</sub> sorption in ACs is physical sorption in nature and the small micropores (in the size range of 0.6–0.9 nm) play the dominant role for the sorption capacity [7,17]. A number of studies demonstrated the importance of small micropores. Mandoki et al. [18] reported that H<sub>2</sub> uptake in ACs is directly proportional to the volumes of small micropores characterized by CO<sub>2</sub> sorption at 273 K. Yushin et al. [19] studied H<sub>2</sub> storage on ACs derived from high-temperature

chlorination of carbides (referred to as CDC) and found that H<sub>2</sub> sorption capacity at 77 K followed the linear relation with volume of small micropores (<1 nm). The CDC with a H<sub>2</sub> capacity of 2.8 wt% (at 1 bar and 77 K) has the maximum volume of small micropores (0.52 cm<sup>3</sup>/g). Guan et al. [20] recently reported the advantages of CO<sub>2</sub> sorption in characterizing such small micropores in TCs.

This article will investigate H<sub>2</sub> sorption in a TC. The porous structure of the TC is characterized using the sorption isotherms of different gas adsorbates and examined by the isosteric heat of adsorption of H<sub>2</sub>.

## 2. Experiments

The TC was prepared with the following procedures: (1) impregnating poly furfuryl alcohol (PFA) in ammonium-form zeolite Y (NH<sub>4</sub>Y form, SiO<sub>2</sub>/Al<sub>2</sub>O<sub>3</sub> = 5.1, by Zeolyst international®), (2) pyrolysis at 1323 K in N<sub>2</sub> flow stream, and (3) acid wash to remove the template zeolite. The detailed preparation procedures can be found in the literature [5].

The morphology the TC was studied by XRD, SEM, and TEM. The bulk density was determined by the ASTM method [21]. The sorption isotherms of N<sub>2</sub> and Ar at 77 K and CO<sub>2</sub> at 273 K were measured on a pore and surface analyzer (Quantachrome, Autosorb-1). Prior to isotherm measurements, the samples were degassed overnight at 523 K and under high vacuum. The specific surface area (*S*<sub>BET</sub>) of the TC was derived using BET method in the pressure range (*P*/*P*<sub>0</sub> = 0.05–0.3). The pore size distribution was derived from the isotherms via the non-local density functional theory (NLDFT) with the assumption that the pores are slit-shaped and the adsorbate–pore interaction is dispersive (for N<sub>2</sub> and Ar).

\* Corresponding author. Tel.: +65 6790 6740; fax: +65 6794 7553.  
E-mail address: [mkwang@ntu.edu.sg](mailto:mkwang@ntu.edu.sg) (K. Wang).

**Table 1**The synthetic conditions and H<sub>2</sub> sorption properties of templated carbons.

Template	Carbon source	Pyrolysis temperature (K)	Hydrogen sorption			Ref.
			wt%	T (K)	P (bar)	
SBA-15 silica	Sucrose	1073	2.0	77	0.9	[10]
Zeolite NaY	Propylene, butylenes	993–1033	2.0	77	1	[9]
Zeolite $\beta$	Acetonitrile	1123	2.6	77	1	[11]
Zeolite $\beta$	Acetonitrile	1123	6.9	77	20	[11]
SBA-15 silica	Acetonitrile	1173	3.4	77	20	[13]
Zeolite Y	Acetonitrile	1073	4.5	77	20	[14]
Silica aerosol	Sucrose	1173	2.0	77	1.1	[15]
MCM-48	Sucrose	1173	2.2	77	1	[16]

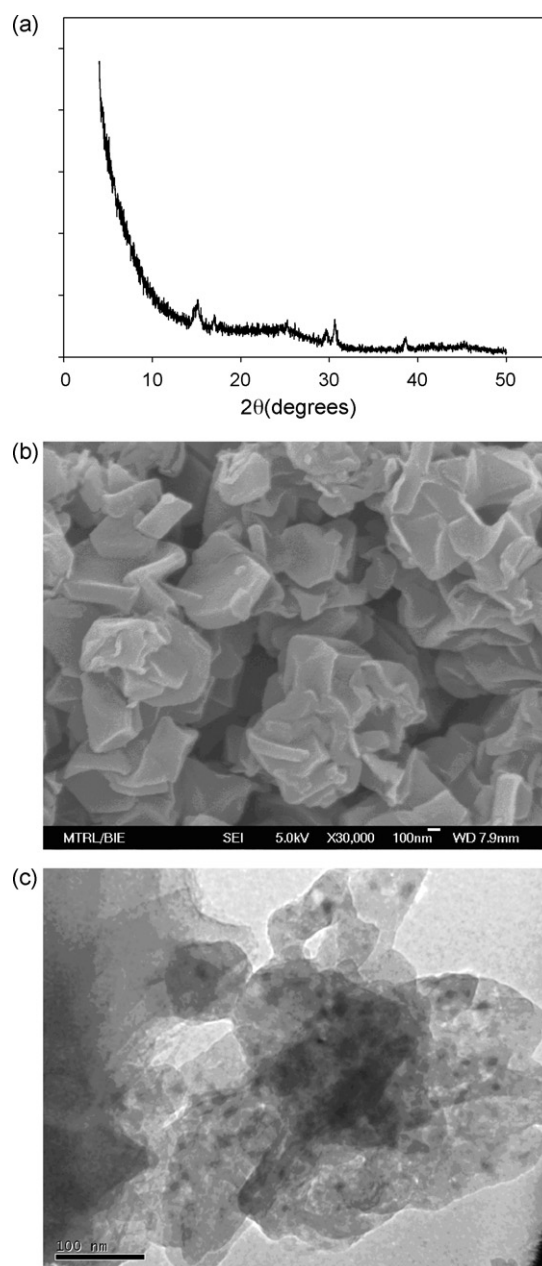
H<sub>2</sub> sorption was measured at three temperatures, 77 K (liquid N<sub>2</sub> temperature), 195 K (dry ice temperature), and 303 K (room temperature), respectively, at the pressure up to 50 bar. H<sub>2</sub> isotherm at 77 K was measured with the pore and surface analyzer up to 1 bar and with a high pressure volumetric rig up to 50 bar. About 0.7 g of TC sample was loaded in the sample cell of the high pressure rig. H<sub>2</sub> gas (purity >99.9%) was supplied by SOXIAL Singapore. During the sorption measurement, the sample cell was submerged in a thermal bath with the controlled temperature.

### 3. Results and discussion

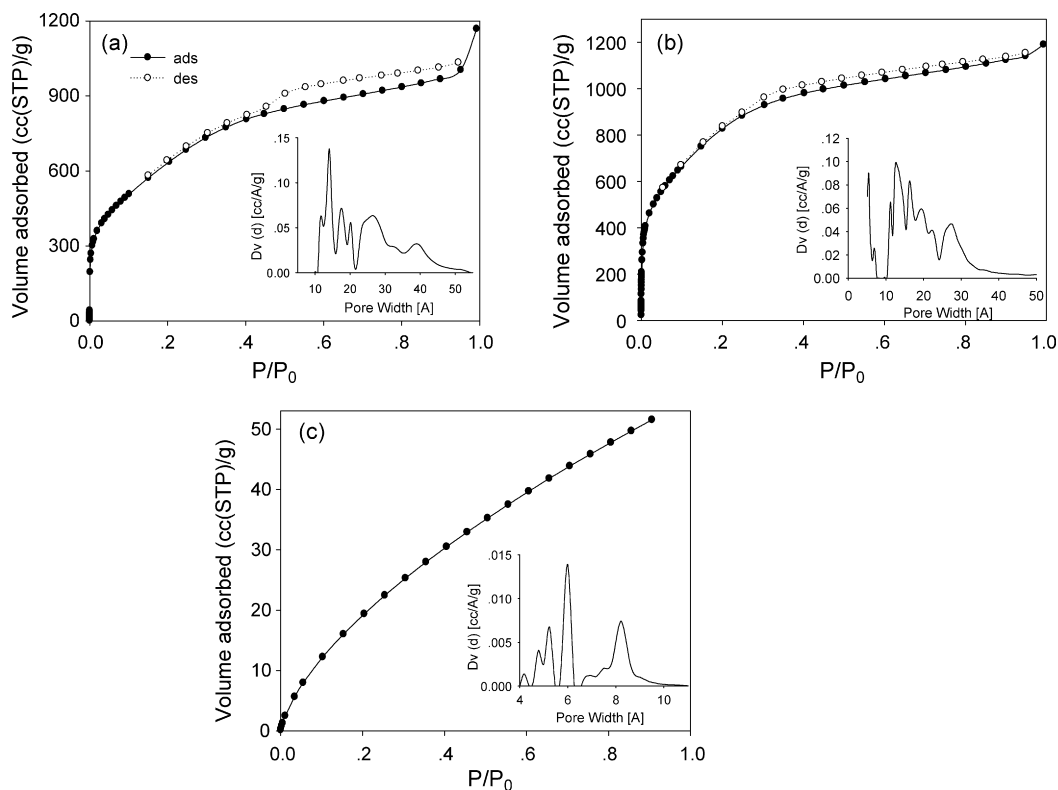
Fig. 1a shows the XRD pattern of the TC. The sample does not exhibit the diffraction peak at 6° (2 $\theta$ ) corresponding to the {1 1 1} plane of zeolite Y. The diffraction peak at 26° (2 $\theta$ ), which corresponds to the {0 0 2} diffraction of graphitic carbon, is very weak as well. These observations suggest that the TC is essentially amorphous in structure. Fig. 1b presents the FESEM image of the TC, which verifies that the graphite crystals are basically amorphous with large interparticle voids (confirmed by the measured ASTM density of 0.28 g/cc). The TEM image (Fig. 1c) further reveals that the graphite crystals have the heterogeneous surface with significant defects.

Fig. 2a shows N<sub>2</sub> isotherm measured at 77 K. The hysteresis in the desorption isotherm suggests the existence of mesopores. The PSD derived via NLDFT was embedded in Fig. 2a. A major micropore peak was seen at ~1.3 nm and two mesopore peaks were found at 2.6 and 3.8 nm, respectively. The micropore peak at 1.3 nm is corresponding to the periodicity of the microchannels of the zeolite template [4,5], while the micropores with the smaller sizes were likely developed by the pyrolysis process. The mesopores were formed probably due to (1) the incomplete infiltration of the carbon precursor into the microchannels [3,5] and (2) the carbonization process. Fig. 2b presents Ar isotherm measured at 77 K and the derived PSD. It is interesting to see that Ar isotherm predicts a higher distribution density of micropores (at ~1.3 nm) as well as a peak of small micropores at ~0.6–0.7 nm, which was undetected by N<sub>2</sub> sorption. Compared with N<sub>2</sub> molecule, Ar is an inert monoatomic gas with smaller molecular dimension and higher critical temperature (150.9 K). These properties enable Ar molecules to penetrate the small micropores with faster kinetics and less diffusion barriers so that the small micropores (as well as the ink-bottled pores) were better probed. Therefore, the BET surface area derived from Ar isotherm (2545 m<sup>2</sup>/g) is the more realistic surface property of the TC for this application. Next, CO<sub>2</sub> isotherm measured at 273 K was studied. CO<sub>2</sub> molecules are assumed to be a 3-centered fluid with both dispersive and electrostatic interaction between the fluid molecules [22]. Fig. 2c shows CO<sub>2</sub> isotherm with the embedded PSD. We see that CO<sub>2</sub> sorption reports three micropore peaks, located at the pore size of 0.5, 0.6, and 0.85 nm, respectively. The micropore peaks at 0.6–0.85 nm were partly agreed by the PSD derived

from Ar sorption (Fig. 2b). It should be noted that, in the measurements of three isotherms, the lowest sorption pressure was set at ~0.005 Torr. It might be possible for Ar or even N<sub>2</sub> molecule to detect the small micropores, but considerably lower sorption pres-



**Fig. 1.** The structure of the TC: (a) XRD, (b) FESEM and (c) TEM.



**Fig. 2.** Sorption isotherm and PSD on the TC: (a)  $N_2$  isotherm at 77 K and the derived PSD; (b) Ar isotherm at 77 K and the derived PSD and (c)  $CO_2$  isotherm at 273 K and the derived PSD.

sure will be required (e.g.  $<10^{-5}$  Torr). The measurement under such conditions will take extremely long time and the results can also be unstable at such a low pressure. Therefore, this exercise confirms our previous findings with another TC that  $CO_2$  sorption is a more reliable method for the characterization of small micropores [20]. This is expected as  $CO_2$  molecule is more strongly adsorbed and smaller in dimension (at the favorable orientation) than  $N_2$  and Ar molecules. This result is also in agreement with the study by Sweatman and Quirke [23] that  $N_2$  sorption at 77 K is diffusion limited or even frozen in such small micropores.

The surface properties of the TC were derived from the three sorption isotherms and listed in Table 2. We see that Ar sorption predicts a slightly higher surface area and a larger micropore volume than  $N_2$ . This is due to the better accessibility of Ar molecules in the porous network of the TC. The difference in the BET areas

detected by molecules with different dimensions was also observed in our previous experiments and attributed to the effect of size exclusion [24].  $CO_2$  sorption reports a very small BET surface area ( $125 \text{ m}^2/\text{g}$ ) and a small micropore volume ( $0.03 \text{ cc/g}$  by DR plot) because the sorption pressure is low ( $\leq 1$  bar). Considerably high sorption pressure is needed for  $CO_2$  molecule to detect the large pores of the TC [22], which is well beyond the working range of the commercial pore and surface analyzer. The high surface area and good micropore volume suggests that the TC is a good candidate for energy storage. The existence of the mesopore volume means that its storage capacity can be further improved.

Fig. 3a shows  $H_2$  isotherm at three temperatures as symbols. Some discrepancy was seen between  $H_2$  isotherm measured on the low pressure rig (at 77 K,  $<1$  bar) and that measured on the high pressure volumetric rig (77 K, 0.3–50 bar), but the agreement

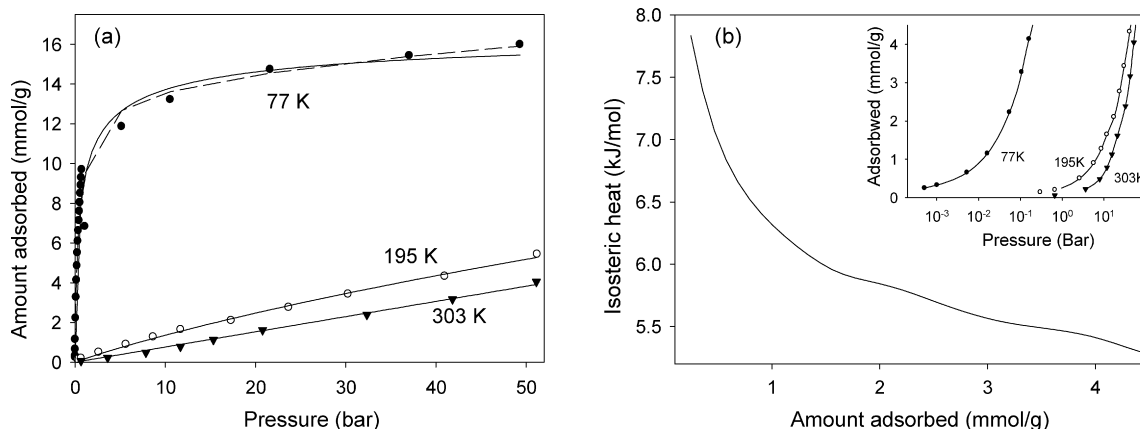


**Fig. 3.**  $H_2$  sorption isotherms and isosteric heat on the TC: (a)  $H_2$  isotherms at three temperatures. Solid line = Toth model ( $C_{as} = 17.3 \text{ mmol/g}$ ,  $b = 8.66 \text{ kPa}^{-1}$ ,  $t = 0.474$ , at 77 K); Dashed line is Nguyen and Do's model; (b) isosteric heat of  $H_2$  sorption on the TC. The embedded figure is the isotherm data involved in the computation.

**Table 2**The surface properties of the TC from N<sub>2</sub>, Ar and CO<sub>2</sub> sorption isotherms.

	$S_{\text{BET}}$ (m <sup>2</sup> /g)	Micropore volume (cc/g)	Total pore volume (cc/g)
N <sub>2</sub>	2136	1.034	1.556
Ar	2545	1.129	1.402
CO <sub>2</sub>	125.0	0.03	0.03

was reasonable. At 77 K, H<sub>2</sub> sorption increases quickly until 10 bar with a capacity of 12 mmol/g (~2.4 wt%). This capacity increases to ~3.1 wt% at the pressure of 50 bar. The capacity is seen to decrease significantly at the dry ice and room temperatures (~0.8 wt% at room temperature and 50 bar). Compared with other storage technologies such as metal-organic framework or metal hydrates, H<sub>2</sub> capacity of TC is comparable but at the lower end. For example, the above-mentioned two technologies reported storage capacities of 6.9 wt% on MOF-5 (77 K and 100 bar) [25] and 5.6 wt% on MgH<sub>2</sub>/2LiNiH<sub>2</sub> [26], respectively. However, physical adsorption in carbonaceous adsorbent presents such advantages of low cost, good reversibility, and safety.

The H<sub>2</sub> isotherms were then fitted, respectively, to the Toth equation,  $C_{\mu} = C_{\mu s} b P / [1 + (b P)^t]^{1/t}$ . The fittings were shown in Fig. 3a as solid lines while the optimal parameters (for the data at 77 K only) were listed in the figure caption. The isotherm parameter ( $t=0.474$ ) indicates that the TC is heterogeneous towards H<sub>2</sub> molecules at 77 K.

The H<sub>2</sub> isosteric heat of adsorption,  $Q_{\text{iso}}$ , was calculated using the Clausius–Clapeyron equation [ $Q_{\text{iso}}/RT^2 = -(\partial \ln P / \partial T)_q$ ] and plotted in Fig. 3b versus the surface loading. The experimental data involved in the computation was plotted in the embedded figure. It is seen that the heat of adsorption drops quickly from ~7.8 to 5 kJ/mol as the surface loading increase to 4 mmol/g. The high value of  $Q_{\text{iso}}$  is an indication of H<sub>2</sub> sorption in small micropores (0.6–0.9 nm) which is mainly responsible for H<sub>2</sub> sorption capacity [8,10,11,24] at ambient temperature. According to Table 2, only about 3% of the total micropore volume of the TC belongs to small micropores. Future efforts should be devoted to increase this volume fraction, rather than to further increase the specific surface area.

Finally, the TC was characterized by H<sub>2</sub> sorption isotherm at 77 K with the model proposed by Nguyen and Do [27]. The model employs isotherm data at supercritical temperature and over a wide pressure range and has been used for the structural characterization of activated carbons, carbon molecular sieves, and carbon membranes [28]. The model fitting to the isotherm data was listed in Fig. 3a as the dashed lines while the distribution of sorption capacities in pores of various dimensions were presented schematically in Fig. 4. We see that the model correctly predicts the small

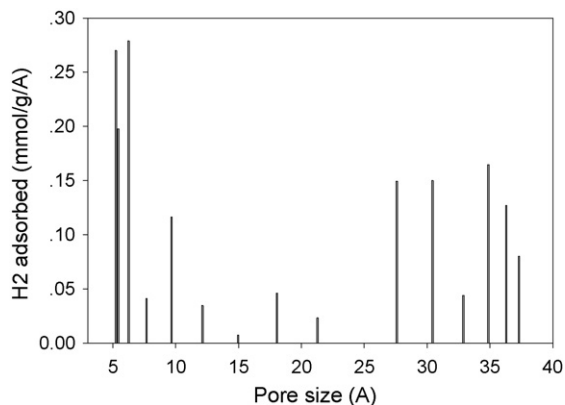


**Fig. 4.** The distribution of the H<sub>2</sub> sorption capacity of the TC derived by Cuong and Do's model.

micropore peaks at 0.5–1 nm (detected by CO<sub>2</sub> sorption) and the mesopore peaks at 3–4 nm (detected by N<sub>2</sub> sorption), although the contribution of the mesopores seems a bit high.

#### 4. Conclusions

The templated carbon synthesized using zeolite Y as template and PFA as carbon source presents a H<sub>2</sub> sorption capacity of 2.4 wt% at 77 K and 10 bar. The carbon contains a small fraction of small micropores which result in an isosteric heat of adsorption of 7.8 kJ/mol. The structure of the carbon was characterized with the sorption isotherm of different adsorbates (Ar, N<sub>2</sub> and CO<sub>2</sub>). CO<sub>2</sub> isotherm at 273 K and Ar isotherm at 77 K were found to be more reliable methods in characterizing the small micropores and the specific surface area, respectively.

#### References

- [1] Z. Ma, T. Kyotani, A. Tomita, Preparation of a high surface area microporous carbon having the structural regularity of Y zeolite, *Chem. Commun.* (2000) 2365–2366.
- [2] Z. Ma, T. Kyotani, Z. Liu, O. Terasaki, A. Tomita, Very high surface area microporous carbon with a 3-D nano-array structure: synthesis and its molecular structure, *Chem. Mater.* 13 (2001) 4413–4415.
- [3] W. Guo, F. Su, X. Zhao, Ordered mesostructured carbon templated by SBA-16 silica, *Carbon* 43 (2005) 2423–2426.
- [4] T. Kyotani, Z. Ma, A. Tomita, Template synthesis of novel porous carbons using various types of zeolites, *Carbon* 41 (2003) 1451–1459.
- [5] F. Su, X.S. Zhao, L. Lv, Z. Zhou, Synthesis and characterization of microporous carbons templated by ammonium-form zeolite Y, *Carbon* 42 (2004) 2821–2831.
- [6] B. Sakintuna, Y. Yurum, Templated porous carbons: a review article, *Ind. Eng. Chem. Res.* 44 (2005) 2893–2902.
- [7] R. Strobel, J. Garche, P.T. Moseley, L. Jorissen, G. Wolf, Hydrogen storage by carbon materials, *J. Power Sources* 159 (2006) 781–801.
- [8] S.K. Bhatia, A.L. Myers, Optimum conditions for adsorptive storage, *Langmuir* 22 (2006) 1688–1700.
- [9] L. Chen, R.K. Singh, P. Webley, Synthesis, characterization and hydrogen storage properties of microporous carbons templated by cation exchanged forms of zeolite Y with propylene and butylene as carbon precursors, *Micropor. Mesopor. Mater.* 102 (2007) 159–170.
- [10] M. Armandi, B. Bonelli, C.O. Arean, E. Garrone, Role of microporosity in hydrogen adsorption on templated nanoporous carbons, *Micropor. Mesopor. Mater.* 112 (2008) 411–418.
- [11] Z. Yang, Y. Xia, R. Mokaya, Enhanced hydrogen storage capacity of high surface area zeolite-like carbon materials, *J. Am. Chem. Soc.* 129 (2007) 1673–1679.
- [12] A. Lachawiec, R.T. Yang, Isotope tracer study of hydrogen spillover on carbon-based adsorbents for hydrogen storage, *Langmuir* 24 (2008) 6159–6165.
- [13] Y. Xia, R. Mokaya, Ordered mesoporous carbon monoliths: CVD nanocasting and hydrogen storage properties, *J. Phys. Chem. C* 111 (2007) 10035–10039.
- [14] Z. Yang, Y. Xia, X. Sun, R. Mokaya, Preparation and hydrogen storage properties of zeolite-templated carbon materials nanocast via chemical vapor deposition: effect of the zeolite template and nitrogen doping, *J. Phys. Chem. B* 110 (2006) 18424–18431.
- [15] Q. Hu, Y. Lu, G.P. Meisner, Preparation of nanoporous carbon particles and their cryogenic hydrogen storage capacities, *J. Phys. Chem. C* 112 (2008) 1516–1523.
- [16] K. Xia, Q. Gao, S. Song, C. Wu, J. Jiang, J. Hu, L. Gao, CO<sub>2</sub> activation of ordered porous carbon CMK-1 for hydrogen storage, *Int. J. Hydrogen Energy* 33 (2008) 116–123.
- [17] Q. Wang, J.K. Johnson, Molecular simulation of hydrogen adsorption in single-walled carbon nanotubes and idealized carbon slit pores, *J. Chem. Phys.* 110 (1999) 577–586.
- [18] N.T. Mandoki, J. Dentzer, T. Piquero, S. Saadallah, P. David, C. Vix-Guterl, Hydrogen storage in activated carbon materials: role of the nanoporous texture, *Carbon* 42 (2004) 2744–2747.
- [19] G. Yushin, R. Dash, J. Jagiello, J. Fischer, Y. Gogotsi, Carbide-derived carbons: effect of pore size on hydrogen uptake and heat of adsorption, *Adv. Funct. Mater.* 16 (2006) 2288–2293.
- [20] C. Guan, K. Wang, C. Yang, X.S. Zhao, Characterization of a zeolite-templated carbon for H<sub>2</sub> storage application, *Micropor. Mesopor. Mater.* 118 (2009) 503–507.
- [21] M.J. Prauchner, R.R. Francisco, Preparation of granular activated carbons for adsorption of natural gas, *Micropor. Mesopor. Mater.* 109 (2008) 581–584.
- [22] E. Pantatosaki, D. Psomadopoulos, T. Steriotis, A.K. Stubos, A. Papaioannou, G.K. Papadopoulos, Micropore size distributions from CO<sub>2</sub> using grand canonical Monte Carlo at ambient temperatures: cylindrical versus slit pore geometries, *Colloid Surf. A: Physicochem. Eng. Aspects* 241 (2004) 127–135.
- [23] M.B. Sweatman, N. Quirke, Characterization of porous materials by gas adsorption: comparison of nitrogen at 77 K and carbon dioxide at 298 K for activated carbon, *Langmuir* 17 (2001) 5011–5020.
- [24] C. Guan, F. Su, X.S. Zhao, K. Wang, Methane storage in a template-synthesized carbon, *Sep. Purif. Tech.* 64 (2008) 124–126.

- [25] D. Saha, Z. Wei, S. Deng, Hydrogen adsorption equilibrium and kinetics in metal-organic framework (MOF-5) synthesized with DEF approach, *Sep. Purif. Tech.* 64 (2009) 280–287.
- [26] W. Luo, (LiNH<sub>2</sub>–MgH<sub>2</sub>): a viable hydrogen storage system, *J. Alloys Compd.* 381 (2004) 284–287.
- [27] C. Nguyen, D.D. Do, Adsorption of supercritical gases in porous media: determination of micropore size distribution, *J. Phys. Chem. B* 103 (1999) 6900–6908.
- [28] C. Nguyen, D.D. Do, K. Haraya, K. Wang, The structural characterization of carbon molecular sieve membrane (CMSM) via gas adsorption, *J. Membr. Sci.* 220 (2003) 177–182.